





Article

Geometric Modeling Using New Cubic Trigonometric B-Spline Functions with Shape Parameter

Abdul Majeed ¹, Muhammad Abbas ^{2,*}, Faiza Qayyum ¹, Kenjiro T. Miura ³,
Md Yushalify Misro ^{4,*} and Tahir Nazir ²

¹ Department of Mathematics, Division of Science and Technology, University of Education, Lahore 54770, Pakistan; abdulmajeed@ue.edu.pk (A.M.); uzmaqayyum.uqk@gmail.com (F.Q.)

² Department of Mathematics, University of Sargodha, Sargodha 40100, Pakistan; tahir.nazir@uos.edu.pk

³ Department of Mechanical Engineering, Shizuoka University, Hamamatsu, Shizuoka 432-8011, Japan; miura.kenjiro@shizuoka.ac.jp

⁴ School of Mathematical Sciences, Universiti Sains Malaysia, Penang 11800, Malaysia

* Correspondence: muhammad.abbas@uos.edu.pk (M.A.); yushalify@usm.my (M.Y.M.)

Received: 5 September 2020; Accepted: 19 October 2020; Published: 24 November 2020



Abstract: Trigonometric B-spline curves with shape parameters are equally important and useful for modeling in Computer-Aided Geometric Design (CAGD) like classical B-spline curves. This paper introduces the cubic polynomial and rational cubic B-spline curves using new cubic basis functions with shape parameter $\zeta \in [0, 4]$. All geometric characteristics of the proposed Trigonometric B-spline curves are similar to the classical B-spline, but the shape-adjustable is additional quality that the classical B-spline curves does not hold. The properties of these bases are similar to classical B-spline basis and have been delineated. Furthermore, uniform and non-uniform rational B-spline basis are also presented. C^3 and C^5 continuities for trigonometric B-spline basis and C^3 continuities for rational basis are derived. In order to legitimize our proposed scheme for both basis, floating and periodic curves are constructed. 2D and 3D models are also constructed using proposed curves.

Keywords: cubic trigonometric b-spline functions; cubic curves and its properties; C^3 and C^5 continuity; geometric modeling

1. Introduction

Splines are a kind of curve, initially evolved in the days prior to computer modeling. Geometric modeling refers to a set of techniques concerned mainly with developing efficient representations of geometric aspects of design. Therefore, geometric modeling is a fundamental part of all CAD (computer-aided design) tools. The basic geometric modeling approaches available to designers on the CAD system are: (1) Wireframe modeling, (2) curve modeling, (3) surface modeling, and (4) solid modeling.

In curve modeling, we deal with trigonometric Bézier-like [1–5], Q-Bézier [6], H-Bézier [7], Ball Bézier-like [8], S- λ Bézier-like [9], classical Bézier, B-spline, and NURBS curve, etc. Schoenberg introduced the trigonometric spline interpolation, spline interpolation of higher derivatives, interpolating spline as limit of polynomials, and Spline interpolation and best quadrature formulae in [10–13]. Lyche and Winther [14] proved a stable recurrence relation for trigonometric B-splines. Walz [15] constructed some identities for trigonometric B-splines with an application to curve design. The term B-spline (Basis spline) introduced is in [16–18]. The curves swarmed the area of Computer Aided Geometric Design (CAGD) in the middle of 1980s. In CAGD, trigonometric polynomials have also procured the great attention for 2D and 3D modeling, for example [19] proposed C^n continuous trigonometric spline curves for data interpolation. The trigonometric Bézier-like curve with shape

parameters based on new trigonometric basis function is proposed by [20]. Majeed and Faiza [21] proposed the curves and bases based on trigonometric B-spline for geometric modeling.

The quadratic trigonometric polynomial curve with C^1 continuity is introduced by [22]. It holds the basic properties of classical B-spline curves. Han [23] added cubic trigonometric B-spline curves on uniform and non-uniform knots with shape parameters to the literature. The application of the B-spline curve in Bio-modeling is given in [24]. Chouby and Ojha [25] introduced the quadratic spline curve with variable shape parameters. Pagani and Scott [26] proposed the sampling method for the reconstruction of curves and surfaces. Surface reconstruction by parallel curves is proposed by [27] with the application of fracture reconstruction.

Hu et al. [28] proposed a scheme based on $\lambda\mu$ -B-spline for the construction of rotational surface. Rational Bézier curves is proposed by [29] for the construction of frontal bone fracture. Yan and Liang [30] proposed algebraic-trigonometric blended spline curve (xyB curves). In the proposed curve, x and y are shape parameters to control the curve. Troll [31] proposed cubic trigonometric Bézier curves. A generation of convex polygon triangulation based on planted trivalent binary tree and ballot notation was proposed by [32]. SARACEVIC and SELİMİ [33] proposed the method for Catalan number decomposition in the expressions of the form $(2 + \iota)$. The authors in [34] have discussed the geometric effect of shape parameter introduced in [22,23]. The trigonometric cubic Bézier curve is proposed by [35] with shape parameters. Gang and Guo-Zhao [36] introduced interpolating α -B-spline build on the new B-splines possessing global and local shape parameters.

This paper presents new trigonometric cubic B-spline basis functions acquiring shape parameter ζ . The proposed basis and curves satisfy the basic properties and are C^5 continuous. Rational basis functions and curves are also derived at uniform and non-uniform knots. C^3 continuous rational curves are also derived in this paper. Validity and applicability of the proposed curves are checked by modeling the floating and periodic curves. In the end, the proposed curves are also used for 2D and 3D modeling. The objectives of the proposed research are:

1. To derive new trigonometric B-spline basis functions with shape parameter ζ ;
2. To derive trigonometric rational B-spline and NURBS curves;
3. To derive different continuities for basis and curve on uniform and non-uniform knots;
4. To apply the derived curves for 2D and 3D modeling.

The rest of the paper is organized as follow. In Section 2, trigonometric B-spine bases have been constructed. Section 3, presents the modeling of cubic trigonometric B-spline curves with its application. Section 4 explains the construction of rational trigonometric B-spline and NURBS bases. The construction of rational trigonometric B-spline curves and geometric modeling with concluding remarks is explained in Section 5.

2. The Construction of Trigonometric B-Spline Basis

The proposed trigonometric cubic B-spline with $\zeta \in [0, 4]$ as shape parameter on knot vector N ($n_0 < n_1 < n_2 < \dots < n_{i+4}$) is defined as:

$$F_j(n) = \begin{cases} a_j(l_3(t_j)) & n \in [n_j, n_{j+1}), \\ \sum_{k=0}^3 c_{j+1,k}(l_k)(t_{j+1}) & n \in [n_{j+1}, n_{j+2}), \\ \sum_{k=0}^3 b_{j+2,k}(l_k)(t_{j+2}) & n \in [n_{j+2}, n_{j+3}), \\ d_{j+3}(l_0(t_{j+3})) & n \in [n_{j+3}, n_{j+4}), \\ 0 & otherwise. \end{cases} \quad (1)$$

Here, $t_j(n) = \frac{\pi}{2}(\frac{n-n_j}{n_{j+1}-n_j})$ and $j \in [0, 4]$. For uniform knots $q_j = q_{j-1} = q_{j-2}$. The functions used in Equation (1) are:

$$\begin{aligned}
 a_j &= \frac{2\alpha_{j-1}\beta_{j-2}q_j^3}{\psi_{j-2}}, b_{j,0} = [1 - (\xi^2 - 3\xi - 1)d_{j+1}]\gamma_{j+1}(q_{j-1} - q_j), \\
 b_{j,1} &= \frac{3\gamma_{j+1}q_{j-1}^2\alpha_j}{2\phi_{j-3}}, \\
 b_{j,2} &= \frac{(1 - 2\xi)\beta_{j-1}q_{j-1}b_{j,0}}{\phi_{j+1}}, \\
 b_{j,3} &= \frac{4\xi[q_{j+1} - q_j]\gamma_j}{\alpha_{j+2}q_j}, \\
 d_j &= \frac{2\beta_{j+1}\psi_{j+2}}{\alpha_{j+2}q_j}, \\
 c_{j,3} &= -\frac{3\beta_{j-1}(q_{j+2} - q_{j-1})[\gamma_{j+2}q_{j+1} + \alpha_{j+1}q_j]a_{j+2}}{4\phi_{j-1}}, \\
 c_{j,2} &= \frac{3\gamma_{j+1}q_{j+1}}{12\gamma_j\alpha_{j+1}q_j^3\psi_{j-1}c_{j,0}}, \\
 c_{j,1} &= \frac{12\gamma_j\alpha_{j+1}q_j^3\psi_{j-1}c_{j,0}}{\phi_{j+1}^2}, \\
 c_{j,0} &= (q_{j+2} - q_{j+1})\alpha_{j+1}d_{j-1},
 \end{aligned}
 \tag{2}$$

where:

$$\begin{aligned}
 q_j &= n_{j+1} - n_j, \alpha_j = \frac{1}{q_{j+1}+q_j}, \beta_j = \frac{1}{q_{j-1}+q_{j-2}} \\
 \gamma_j &= \frac{2}{q_{j-1}+q_j+q_{j+1}}, \phi_j = \frac{\psi_{j-2}(q_{j+1}+1)}{2(\beta_{j-1}q_{j-1}^3+\alpha_jq_{j+1}^2)}, \\
 \psi_j &= 6\xi^2\alpha_{j-1}q_{j-1}^2 - 3\xi q_j + 10\beta_{j+1}q_{j+1}^2.
 \end{aligned}
 \tag{3}$$

The proposed cubic trigonometric B-spline functions possessing ξ are defined as:

$$\begin{aligned}
 l_0(t) &= (1 - \sin t)^2(\xi^2 - \xi + 1 - \sin t), \\
 l_1(t) &= (1 + \cos t)^2(\xi^2 - \xi + 1 + \cos t), \\
 l_2(t) &= (1 + \sin t)^2(\xi^2 - \xi + 1 + \sin t), \\
 l_3(t) &= (1 - \cos t)^2(\xi^2 - \xi + 1 - \cos t).
 \end{aligned}
 \tag{4}$$

The basis functions can be defined on $n \in [n_j, n_{j+1})$ by replacing j by $j - 3, j - 2, j - 1, j$ in Equation (1). The basis of the functions are:

$$\begin{aligned}
 F_0(n) &= d_j(l_0(t_j)), \\
 F_1(n) &= \sum_{k=0}^3 b_{j,k}(l_k)(t_j), \\
 F_2(n) &= \sum_{k=0}^3 c_{j,k}(l_k)(t_j), \\
 F_3(n) &= a_j(l_3(t_j)).
 \end{aligned}
 \tag{5}$$

Figure 1 represents the graphical behavior of spline functions, where the effect of shape parameter ξ is represented in Figure 2.

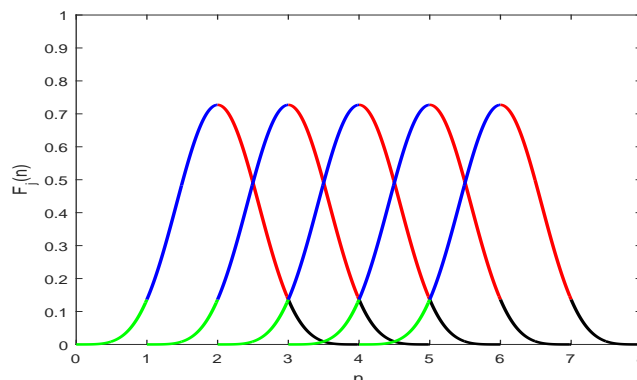


Figure 1. Graphical behavior of the proposed trigonometric functions.

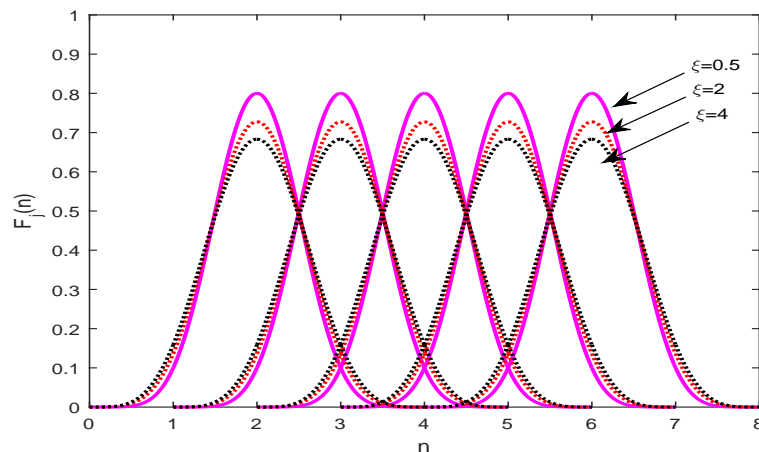


Figure 2. The effect of shape parameter ξ .

Properties of the Cubic Trigonometric Spline Functions

The following properties are satisfied by the proposed basis.

Theorem 1. *The proposed cubic trigonometric B-spline basis function satisfy the partition of unity property:*

$$\sum_{j=0}^3 F_j(n) = 1.$$

Proof of Theorem 1. See Appendix A □

Theorem 2. *The cubic trigonometric B-spline basis holds non-negativity property i.e., $F_j(n) > 0$.*

Proof of Theorem 2. See Appendix B □

Theorem 3. *The derived basis are C^3 and C^5 continuous for non-uniform knots.*

Proof of Theorem 3. See Appendix C □

3. Modeling of Cubic Trigonometric B-Spline Curves

Definition 1. *Let $F_j(n)$ be the basis functions defined in Equation (5) above and $S_j \in R^2$ for $j = [0,3]$ are control points in plane. The cubic trigonometric B-spline curve is defined as:*

$$G(n) = \sum_{j=0}^3 F_j(n)S_j, \tag{6}$$

where,

$$\begin{aligned} F_0(n) &= d_j(l_0(t_j)), \\ F_1(n) &= \sum_{k=0}^3 b_{j,k}(l_k)(t_j), \\ F_2(n) &= \sum_{k=0}^3 c_{j,k}(l_k)(t_j), \\ F_3(n) &= a_j(l_3(t_j)). \end{aligned}$$

and

$$t_j(n) = \frac{\pi}{2} \left(\frac{n - n_j}{n_{j+1} - n_j} \right).$$

3.1. Properties of Cubic Trigonometric B-Spline Curves

The following properties are obeyed by proposed curves.

3.1.1. Convex Hull Property

The constructed curves always lies within the convex hull of the control polygon as shown in Figure 3.

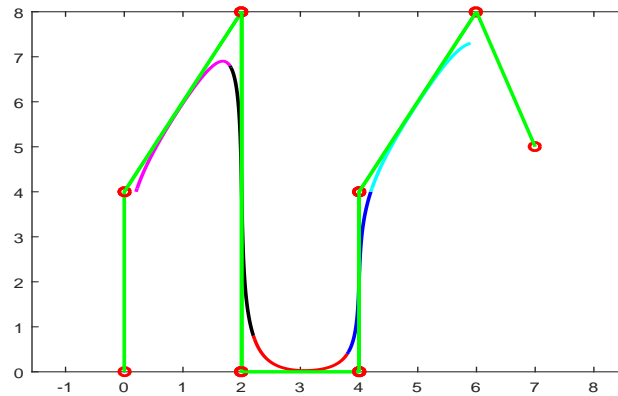


Figure 3. Convex hull property.

3.1.2. Affine Transformation

The transformation may be of rotation, scaling, reflection, and translation. Let L be the transformation then:

$$L\left(\sum_{j=0}^n S_j F_j(n)\right) = \sum_{j=0}^n L(S_j) F_j(n).$$

Theorem 4. The proposed curve possesses C^3 and C^5 continuity for $\xi \neq 1$. For multiple knots, the curve has C^{3-k} continuity here $k = [0,3]$.

Proof of Theorem 4. See Appendix D □

3.2. Floating and Periodic Curves Using Proposed Trigonometric Basis Functions

3.2.1. Floating Cubic B-Spline Curve

The cubic trigonometric basis are used to construct the floating curves with $\xi = 4$ and 1 as shown in Figure 4.

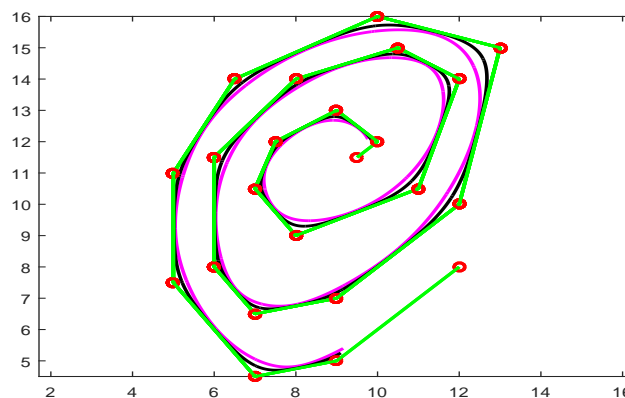


Figure 4. Floating curve using $\xi = 4$ (magenta) and $\xi = 1$ (black) color curve.

3.2.2. Periodic Trigonometric B-Spline Curves

Periodic curve is drawn using cubic trigonometric B-spline basis functions as shown in Figure 5. Periodic curves can be drawn in blue, red, and magenta colors with $\zeta = 0, 2,$ and 4 respectively these shape parameters provide more flexibility than classical B-spline curves.

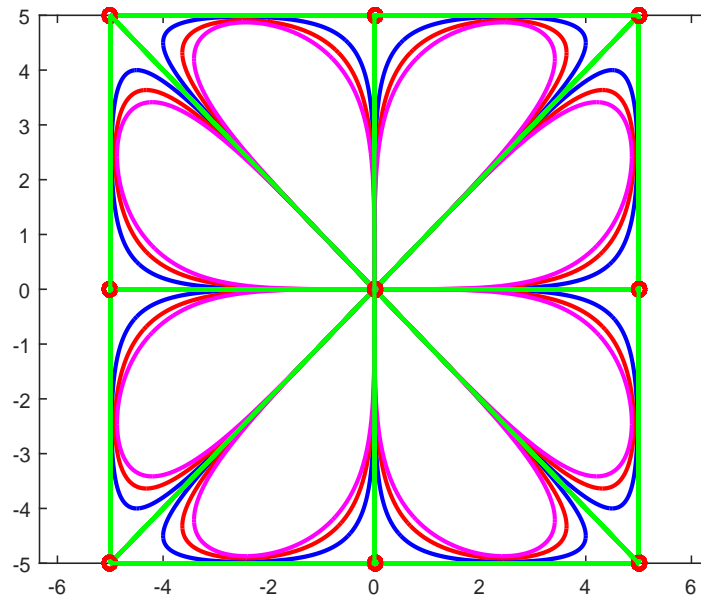


Figure 5. Periodic curve with $\zeta = 0$ (Blue), $\zeta = 2$ (Red), and $\zeta = 4$ (Magenta).

From Figures 4 and 5, it is observed that the proposed cubic trigonometric B-spline curves work well for both floating and periodic curves. It is also observed that shape parameter ζ has a significant effect on the curve.

4. Rational Trigonometric B-Spline and NURBS

Definition 2. Rational trigonometric B-spline and NURBS are a generalization of B-spline basis. It enhances the flexibility of the curve. It is generally expressed as:

$$Y(n) = \frac{\sum_{j=0}^n (w_j F_{j,d}(n))}{\sum_{j=0}^n (w_j F_{j,d}(n))}.$$

Here d is the degree of trigonometric B-spline basis. w_j s are positive weights. $F_{j,d}(n)$ are the trigonometric B-spline basis. Simply, we can write it as:

$$Y(n) = \sum_{j=0}^n Q_{j,d}(n),$$

where,

$$Q_{j,d}(n) = \frac{(w_j F_{j,d}(n))}{\sum_{j=0}^n (w_j F_{j,d}(n))}.$$

The expression for the rational trigonometric B-spline and NURBS becomes:

$$Y(n) = \frac{\sum_{j=0}^3 (w_j F_j(n))}{\sum_{j=0}^3 (w_j F_j(n))}.$$

or

$$Y(n) = \sum_{j=0}^3 Q_j(n),$$

where

$$Q_j(n) = \frac{(w_j F_j(n))}{\sum_{j=0}^3 (w_j F_j(n))}.$$

Remark 1. In the above equations if B-spline basis $F_j(n)$ are defined over uniform knots then the basis becomes Rational trigonometric B-spline otherwise NURBS.

Properties of the Rational Trigonometric B-Spline and NURBS

The proposed rational trigonometric B-spline and NURBS basis possess the following properties.

Theorem 5. For all $w_j = 1$, then $Q_j(n) = F_j(n)$.

Proof of Theorem 5. We prove this by taking:

$$Q_j(n) = \frac{w_j F_j(n)}{\sum_{j=0}^3 (w_j F_j(n))}.$$

Put, $w_j = 1$ then above equation becomes:

$$Q_j(n) = \frac{F_j(n)}{(F_0(n) + F_1(n) + F_2(n) + F_3(n))}.$$

Here $F_0(n), F_1(n), F_2(n), F_3(n)$, are defined in Equation (5). Since, we have proved earlier that:

$$\sum_{j=0}^3 F_j(n) = 1.$$

Thus, we get:

$$Q_j(n) = (F_j(n)).$$

□

Theorem 6. The rational cubic trigonometric B-spline basis function satisfies the partition of unity property i.e.

$$Y(n) = \sum_{j=0}^3 Q_j(n) = 1.$$

Proof of Theorem 6. Since,

$$Q_j(n) = \frac{(w_j F_j(n))}{\sum_{j=0}^3 (w_j F_j(n))},$$

or simply:

$$Q_j(n) = \frac{(w_j F_j(n))}{w_0 F_0(n) + w_1 F_1(n) + w_2 F_2(n) + w_3 F_3(n)}.$$

Now,

$$Y(n) = \sum_{j=0}^3 Q_j(n),$$

$$Y(n) = Q_0(n) + Q_1(n) + Q_2(n) + Q_3(n).$$

$$\begin{aligned}
 Y(n) &= \frac{w_0 F_0(n)}{w_0 F_0(n) + w_1 F_1(n) + w_2 F_2(n) + w_3 F_3(n)} \\
 &+ \frac{w_1 F_1(n)}{w_0 F_0(n) + w_1 F_1(n) + w_2 F_2(n) + w_3 F_3(n)} \\
 &+ \frac{w_2 F_2(n)}{w_0 F_0(n) + w_1 F_1(n) + w_2 F_2(n) + w_3 F_3(n)} \\
 &+ \frac{w_3 F_3(n)}{w_0 F_0(n) + w_1 F_1(n) + w_2 F_2(n) + w_3 F_3(n)}. \\
 &= \frac{w_0 F_0(n) + w_1 F_1(n) + w_2 F_2(n) + w_3 F_3(n)}{w_0 F_0(n) + w_1 F_1(n) + w_2 F_2(n) + w_3 F_3(n)} \\
 &= 1
 \end{aligned}
 \tag{7}$$

Hence, partition of unity holds. □

5. Rational Trigonometric B-Spline and NURBS Curve

Definition 3. Rational trigonometric B-spline and NURBS curve possessing shape parameter ξ is expressed generally as:

$$Z(n) = \frac{\sum_{j=0}^3 (w_j H_j F_j(n))}{\sum_{j=0}^3 (w_j F_j(n))},$$

or

$$Z(n) = \sum_{j=0}^3 H_j Q_j(n),$$

where $H_j = H_0, \dots, H_n$ are control points, w_j s are non-negative weights, and $F_j(n)$ are trigonometric B-spline basis.

5.1. Properties of Rational Trigonometric B-Spline and NURBS Curve

5.1.1. Convex Hull Property

Rational trigonometric B-spline and NURBS curves always lie inside the convex hull of control polygon as shown in Figures 6 and 7, respectively.

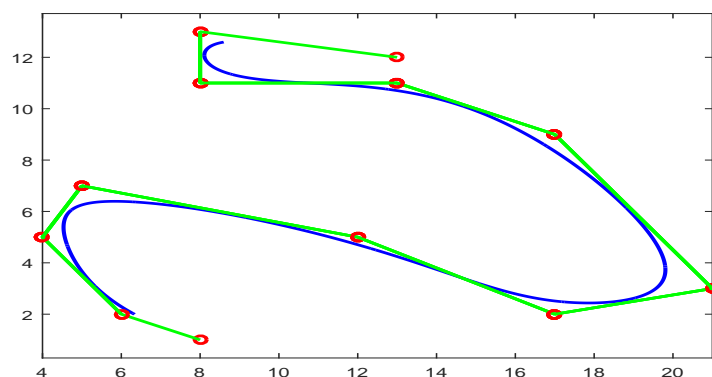


Figure 6. Convex hull of rational trigonometric curve.

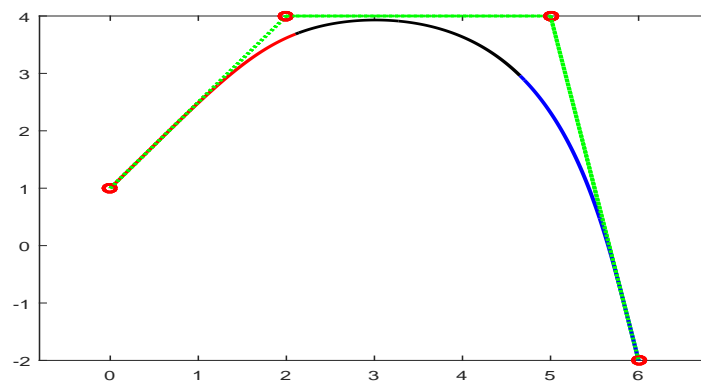


Figure 7. Convex hull of NURBS curve.

5.1.2. Affine Transformation

Let T be an affine transformation, then:

$$T\left(\frac{\sum_{j=0}^n (w_j H_j F_{j,d}(n))}{\sum_{j=0}^n (w_j F_{j,d}(n))}\right) = \frac{\sum_{j=0}^n (w_j T(H_j) F_{j,d}(n))}{\sum_{j=0}^n (w_j F_{j,d}(n))}.$$

5.1.3. Local Approximation

The shape of the curve can be distorted, either by changing the control points or weights. In Figure 8, the curve is without any change of control point and weight. Figure 9 explains that the change of control points affect the curve locally. Similarly, in Figure 10, a change of weight can be seen clearly.

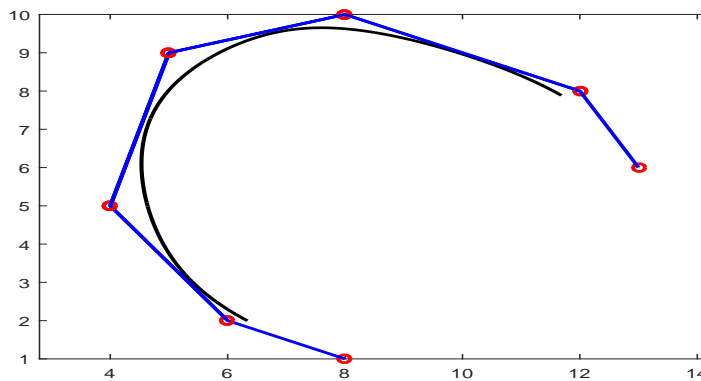


Figure 8. Without changing the weight and control point.

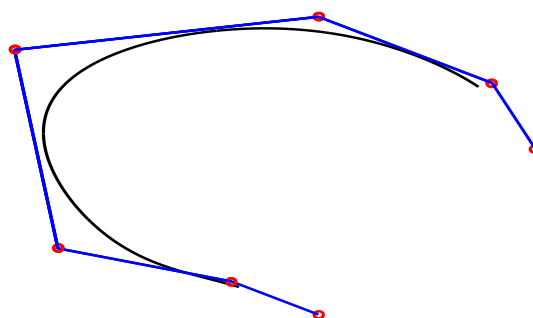


Figure 9. The effect of changing the control point.

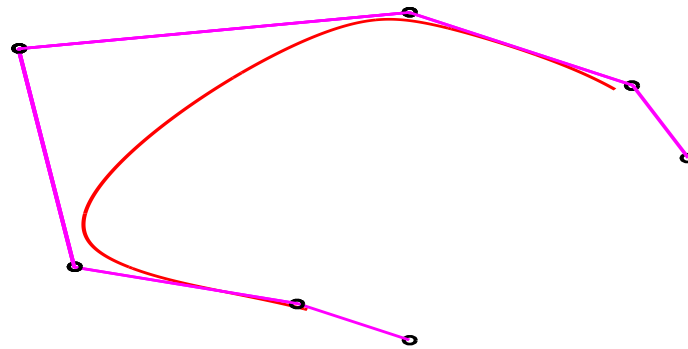


Figure 10. The effect of changing the weight.

5.1.4. Continuity

Theorem 7. *The rational trigonometric B-spline and NURBS curve has C^3 continuity. These curve have C^{3-k} continuity, $k = [0,4]$. The curve becomes discontinuous at $k = 4$.*

Proof of Theorem 7. See Appendix E □

5.2. Floating and Periodic Rational Trigonometric B-Spline and NURBS Curve

5.2.1. Floating Rational and NURBS Curve

A floating curve is also known as an open curve, such curves whose first and last point does not meet. Figures 11 and 12 show the floating rational trigonometric B-spline and NURBS curve, respectively. A total of 36 control points are used to construct rational trigonometric curve possessing $\xi = 3,0$ for the blue and red color, respectively. The control polygon of NURBS is formed possessing $\xi = 3$ see Figure 12.

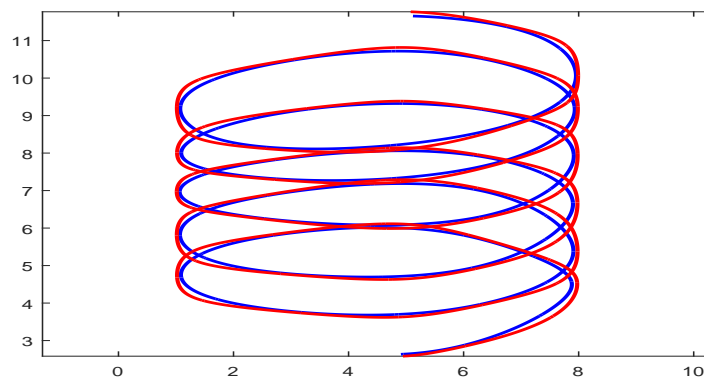


Figure 11. Floating rational trigonometric curve with different ξ .

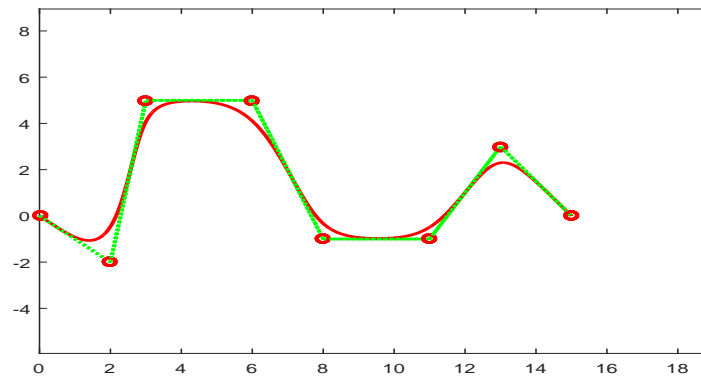


Figure 12. Floating NURBS curve with $\zeta = 3$.

5.2.2. Periodic Rational and NURBS Curve

In Figures 13 and 14 the periodic rational trigonometric B-spline and NURBS curve is constructed. The generated rational trigonometric curve consists of 12 control points.

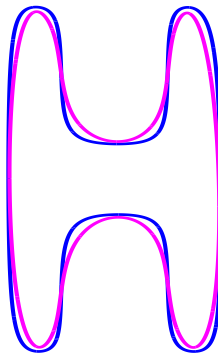


Figure 13. Periodic rational curve with different ζ .

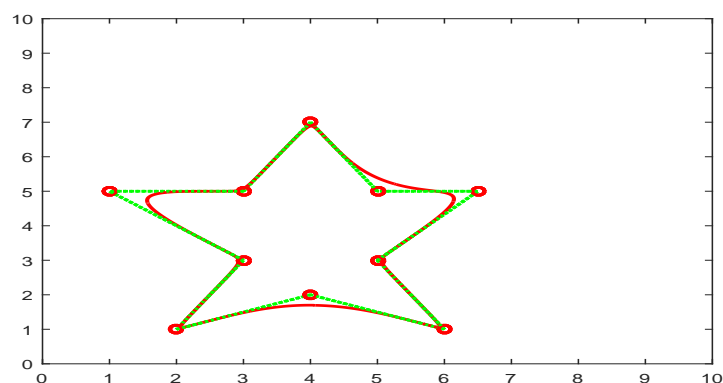


Figure 14. Periodic NURBS curve with $\zeta = 3$.

The shape parameter and weight make the designing of the Rational and NURBS curve more smooth and accurate.

5.3. Application of B-Spline and Uniform Rational Trigonometric B-Spline Curve

Proposed cubic trigonometric curves have been used for 2D and 3D modeling like in Figure 15, and we have designed an aeroplane with 107 control points with the shape parameter $\zeta = 0.4$.

The execution time for this model is 0.578 s. In Figure 16, glass has been designed using 25 control points and $\zeta = 2$. The CPU time recorded for this model is 0.209 s. An apple has been designed in a 2D form using the proposed method as shown in Figure 17. Different control points with $\zeta = 3$ is used for this model. Lastly, proposed curves have been used to design a vase in 3D form as shown in Figure 18. The shape parameter $\zeta = 2$ is used in this model. The execution time for this model is 0.593 s.

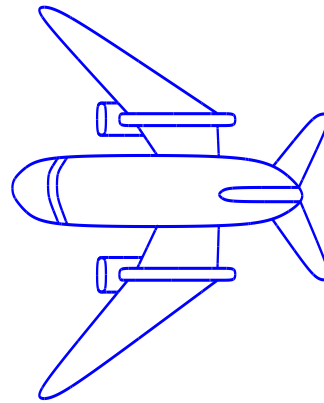


Figure 15. Aeroplane design using cubic trigonometric B-spline curves.

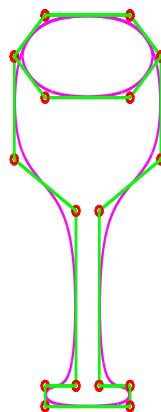


Figure 16. Glass design using cubic trigonometric B-spline curve.

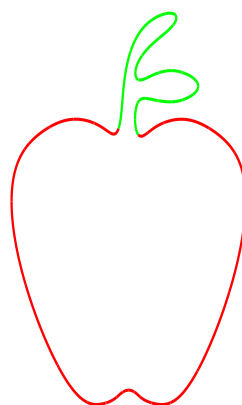


Figure 17. Apple designing using rational B-spline curve.

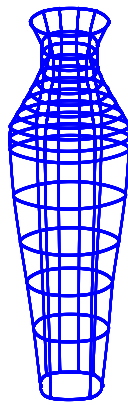


Figure 18. 3D vase mesh design using cubic trigonometric B-spline curves.

5.4. Conclusions

Cubic trigonometric and rational cubic trigonometric B-spline basis functions and curves with shape parameter ζ were derived in this paper. The cubic trigonometric B-spline curves were C^3 and C^5 continuous at uniform and non-uniform knots and were derived. Rational cubic trigonometric B-spline curves were C^3 continuous for both uniform and non-uniform knots. Both cubic polynomial and cubic rational basis and curves obeyed the basic properties and were derived in this paper. The rendering of floating and periodic curves reflected the flexibility and applicability of the proposed method. Different 2D and 3D models were designed using the proposed curves successfully. This curve was more flexible, easy to use, and had a larger parametric range than the existing scheme. This work can be extended by adding shape parameter, using higher degree in functions, and by constructing the surface using proposed curves.

Author Contributions: Methodology, A.M., M.A. and F.Q.; software, A.M., M.A., F.Q., and T.N.; formal analysis, A.M., M.A., F.Q., K.T.M., M.Y.M. and T.N.; writing, original draft preparation, A.M., M.A. and F.Q.; Investigation, A.M., M.A., M.Y.M., and T.N.; writing, review and editing, A.M., M.A., F.Q., K.T.M., M.Y.M. and T.N.; visualization, A.M., M.A., F.Q., K.T.M., M.Y.M. and T.N.; resources, M.A. and K.T.M.; supervision, A.M., M.A. and K.T.M.; funding acquisition, M.A., and K.T.M. All authors have read and agreed to the published version of the manuscript.

Funding: This work was supported by Universiti Sains Malaysia under Short Term Grant 304/PMATHS/6315223.

Acknowledgments: The authors would like to thank the anonymous referees for their careful reading of this manuscript and also for their constructive suggestions which considerably improved the article.

Conflicts of Interest: The authors declare no conflict of interest.

Abbreviations

The following abbreviations are used in this manuscript:

2D	two dimensional
3D	three dimensional
CAD	computer-aided design
NURBS	non-uniform rational B-spline
C^3	parametric continuity of degree three
C^5	parametric continuity of degree five
CPU	central processing unit

Appendix A

Proof. We use basis functions $F_0(n)$, $F_1(n)$, $F_2(n)$ and $F_3(n)$ defined in Equation (5). Thus, we get,

$$\sum_{j=0}^3 F_j(n) = d_j(l_0(t_j)) + \sum_{k=0}^3 b_{j,k}(l_k)(t_j) + \sum_{k=0}^3 c_{j,k}(l_k)(t_j) + a_j(l_3(t_j)).$$

$$\sum_{j=0}^3 F_j(n) = \frac{1}{6\zeta^2 - 6\zeta + 10} (1 - \sin t_j)^2 (\zeta^2 - \zeta + 1 - \sin t_j) \tag{A1}$$

$$+ \frac{1}{6\zeta^2 - 6\zeta + 10} (1 + \cos t_j)^2 (\zeta^2 - \zeta + 1 + \cos t_j)$$

$$+ \frac{1}{6\zeta^2 - 6\zeta + 10} (1 + \sin t_j)^2 (\zeta^2 - \zeta + 1 + \sin t_j)$$

$$+ \frac{1}{6\zeta^2 - 6\zeta + 10} (1 - \cos t_j)^2 (\zeta^2 - \zeta + 1 - \cos t_j).$$

$$\sum_{j=0}^3 F_j(n) = \frac{1}{6\zeta^2 - 6\zeta + 10} (\zeta^2 - \zeta + 1 - (1 + 2(\zeta^2 - \zeta + 1))\sin t_j + (2 + \zeta^2 - \zeta + 1)\sin^2 t_j - \sin^3 t_j)$$

$$+ \frac{1}{6\zeta^2 - 6\zeta + 10} (\zeta^2 - \zeta + 1 + (1 + 2(\zeta^2 - \zeta + 1))\cos t_j + (2 + \zeta^2 - \zeta + 1)\cos^2 t_j + \cos^3 t_j)$$

$$+ \frac{1}{6\zeta^2 - 6\zeta + 10} (\zeta^2 - \zeta + 1 + (1 + 2(\zeta^2 - \zeta + 1))\sin t_j + (2 + \zeta^2 - \zeta + 1)\sin^2 t_j + \sin^3 t_j)$$

$$+ \frac{1}{6\zeta^2 - 6\zeta + 10} (\zeta^2 - \zeta + 1 - (1 + 2(\zeta^2 - \zeta + 1))\cos t_j + (2 + \zeta^2 - \zeta + 1)\cos^2 t_j - \cos^3 t_j).$$

$$\sum_{j=0}^3 F_j(n) = \frac{1}{6\zeta^2 - 6\zeta + 10} [\zeta^2 - \zeta + 1 - (1 + 2(\zeta^2 - \zeta + 1))\sin t_j + (2 + \zeta^2 - \zeta + 1)\sin^2 t_j - \sin^3 t_j$$

$$+ \zeta^2 - \zeta + 1 + (1 + 2(\zeta^2 - \zeta + 1))\cos t_j + (2 + \zeta^2 - \zeta + 1)\cos^2 t_j + \cos^3 t_j$$

$$+ \zeta^2 - \zeta + 1 + (1 + 2(\zeta^2 - \zeta + 1))\sin t_j + (2 + \zeta^2 - \zeta + 1)\sin^2 t_j + \sin^3 t_j$$

$$+ \zeta^2 - \zeta + 1 - (1 + 2(\zeta^2 - \zeta + 1))\cos t_j + (2 + \zeta^2 - \zeta + 1)\cos^2 t_j - \cos^3 t_j].$$

$$\sum_{j=0}^3 F_j(n) = \frac{1}{6\zeta^2 - 6\zeta + 10} [4(\zeta^2 - \zeta + 1) + (2 + \zeta^2 - \zeta + 1) + (2 + \zeta^2 - \zeta + 1)].$$

$$\sum_{j=0}^3 F_j(n) = \frac{1}{6\zeta^2 - 6\zeta + 10} [4(\zeta^2 - \zeta + 1) + 2(2 + \zeta^2 - \zeta + 1)].$$

$$\sum_{j=0}^3 F_j(n) = \frac{1}{6\zeta^2 - 6\zeta + 10} [4\zeta^2 - 4\zeta + 4 + 4 + 2\zeta^2 - \zeta + 2].$$

$$\sum_{j=0}^3 F_j(n) = \frac{1}{6\zeta^2 - 6\zeta + 10} [6\zeta^2 - 6\zeta + 10].$$

$$\sum_{j=0}^3 F_j(n) = 1. \tag{A2}$$

□

Appendix B

Proof. The first and fourth term of equation (1) contains only a single term so $F_j(n) > 0$. The third term involves summation, so we need to show it is either positive or not. For this let $z = \tan \frac{1}{2}t$. Here $t \in [0, 1]$.

$$\sum_{i=0}^3 b_{j+2,i}(l_i(t_{j+2})) = b_{j+2,0}l_0(t_{j+2}) + b_{j+2,1}l_1(t_{j+2}) + b_{j+2,2}l_2(t_{j+2}) + b_{j+2,3}l_3(t_{j+2}).$$

Let $s(\xi) = \xi^2 - \xi + 1$.

$$\begin{aligned} \sum_{i=0}^3 b_{j+2,i}(l_i(t_{j+2})) &= b_{j+2,0}[s(\xi) - (1 + 2(s(\xi)))\sin t_{j+2} + (2 + s(\xi))\sin^2 t_{j+2} - \sin^3 t_{j+2}] \\ &\quad + b_{j+2,1}[s(\xi) + (1 + 2(s(\xi)))\cos t_{j+2} + (2 + s(\xi))\cos^2 t_{j+2} + \cos^3 t_{j+2}] \\ &\quad + b_{j+2,2}[s(\xi) + (1 + 2(s(\xi)))\sin t_{j+2} + (2 + s(\xi))\sin^2 t_{j+2} + \sin^3 t_{j+2}] \\ &\quad + b_{j+2,3}[s(\xi) - (1 + 2(s(\xi)))\cos t_{j+2} + (2 + s(\xi))\cos^2 t_{j+2} - \cos^3 t_{j+2}]. \end{aligned}$$

$$\begin{aligned} \sum_{i=0}^3 b_{j+2,i}(l_i(t_{j+2})) &= (s(\xi))[b_{j+2,0} + b_{j+2,1} + b_{j+2,2} + b_{j+2,3}] \\ &\quad + (1 + 2(s(\xi)))[(b_{j+2,2} - b_{j+2,0})\sin t_{j+2} + (b_{j+2,1} - b_{j+2,3})\cos t_{j+2}] \\ &\quad + (2 + s(\xi))[(b_{j+2,2} + b_{j+2,0})\sin^2 t_{j+2} + (b_{j+2,1} + b_{j+2,3})\cos^2 t_{j+2}] \\ &\quad + [(b_{j+2,2} - b_{j+2,0})\sin^3 t_{j+2} + (b_{j+2,1} - b_{j+2,3})\cos^3 t_{j+2}]. \end{aligned}$$

After substituting $\sin t = \frac{2z}{1+z^2}$, $\cos t = \frac{1-z^2}{1+z^2}$ the equation above becomes

$$\begin{aligned} \sum_{i=0}^3 b_{j+2,i}(l_i(t_{j+2})) &= s(\xi)[b_{j+2,0} + b_{j+2,1} + b_{j+2,2} + b_{j+2,3}] \\ &\quad + (1 + 2(s(\xi)))[(b_{j+2,2} - b_{j+2,0})\left(\frac{2z}{1+z^2}\right) + (b_{j+2,1} - b_{j+2,3})\left(\frac{1-z^2}{1+z^2}\right)] \\ &\quad + (2 + s(\xi))[(b_{j+2,2} + b_{j+2,0})\left(\frac{4z^2}{(1+z^2)^2}\right) + (b_{j+2,1} + b_{j+2,3})\left(\frac{(1-z^2)^2}{(1+z^2)^2}\right)] \\ &\quad + [(b_{j+2,2} - b_{j+2,0})\left(\frac{8z^3}{(1+z^2)^3}\right) + (b_{j+2,1} - b_{j+2,3})\left(\frac{(1-z^2)^3}{(1+z^2)^3}\right)]. \end{aligned}$$

$$\begin{aligned} \sum_{i=0}^3 b_{j+2,i}(l_i(t_{j+2})) &= \left(\frac{1}{1+z^2}\right)^3 [s(\xi)(1+z^2)^3(b_{j+2,0} + b_{j+2,1} + b_{j+2,2} + b_{j+2,3}) \\ &\quad + (1 + 2(s(\xi)))(b_{j+2,2} - b_{j+2,0})(2z)(1+z^2)^2 \\ &\quad + (1 + 2(s(\xi)))(b_{j+2,1} - b_{j+2,3})((1-z^2)(1+z^2)^2) \\ &\quad + (2 + s(\xi))(b_{j+2,2} + b_{j+2,0})((4z^2)(1+z^2)) \\ &\quad + (b_{j+2,1} + b_{j+2,3})((1-z^2)^2(1+z^2)) \\ &\quad + (b_{j+2,2} - b_{j+2,0})(8z^3) \\ &\quad + (b_{j+2,1} - b_{j+2,3})((1-z^2)^3)]. \end{aligned}$$

Comparing the coefficients of $z^6, z^5, z^4, z^3, z^2, z$ and constants, we get:

$$\begin{aligned} \sum_{i=0}^3 b_{j+2,i}(l_i(t_{j+2})) = & \{[(s(\xi))(b_{j+2,0} + b_{j+2,2}) + 2(1 + 2s(\xi))b_{j+2,3} + 2b_{j+2,1}]z^6 \\ & + (2(1 + 2(s(\xi)))(b_{j+2,2} - b_{j+2,0}))z^5 \\ & + ((8 + 7(s(\xi)))(b_{j+2,0} + b_{j+2,2}) + 4(s(\xi) - 1)b_{j+2,3})z^4 \\ & + (4(2s(\xi) + 3)(b_{j+2,2} - b_{j+2,0}))z^3 \\ & + ((8 + 7s(\xi))(b_{j+2,0} + b_{j+2,2}) + 4(s(\xi) - 1)b_{j+2,1})z^2 \\ & + (2(1 + 2s(\xi))(b_{j+2,2} - b_{j+2,0}))z \\ & + s(\xi)(b_{j+2,0} + b_{j+2,2}) + 4(s(\xi) + 1)b_{j+2,1}\}. \end{aligned}$$

From the above equation, we get:

$$\sum_{k=0}^6 \left(\frac{1}{(1 + z^2)^3}\right) [y_k z^k] > 0 \text{ for all } z \in [0, 1).$$

Here,

$$\begin{aligned} y_0 &= s(\xi)(b_{j+2,0} + b_{j+2,2}) + 4(s(\xi) + 1)b_{j+2,1}, \\ y_1 &= 2(1 + 2s(\xi))(b_{j+2,2} - b_{j+2,0}), \\ y_2 &= (8 + 7s(\xi))(b_{j+2,0} + b_{j+2,2}) + 4(s(\xi) - 1)b_{j+2,1}, \\ y_3 &= 4(3 + 2s(\xi))(b_{j+2,2} - b_{j+2,0}), \\ y_4 &= (8 + 7s(\xi))(b_{j+2,0} + b_{j+2,2}) + 4(s(\xi) - 1)b_{j+2,3}, \\ y_5 &= 2(1 + 2s(\xi))(b_{j+2,2} - b_{j+2,0}), \\ y_6 &= s(\xi)(b_{j+2,2} + b_{j+2,0}) + 2(1 + 2s(\xi))b_{j+2,3} + 2b_{j+2,1}. \end{aligned}$$

The theorem clearly follows for $n \in [n_{j+1}, n_{j+2})$. \square

Appendix C

Proof. In the knot interval $n \in [n_j, n_{j+1})$, the derivatives are taken at knot n_{j+1}^- of equation (1) as:

$$\begin{aligned} F_j(n_{j+1}^-) &= s(\xi)a_j. \\ F'_j(n_{j+1}^-) &= \left(\frac{\pi}{2}\right)(1 + 2s(\xi))a_j. \\ F''_j(n_{j+1}^-) &= \left(\frac{\pi}{2}\right)^2(2 + s(\xi))a_j. \\ F'''_j(n_{j+1}^-) &= \left(\frac{\pi}{2}\right)^3(5 - 2s(\xi))a_j. \\ F^{iv}_j(n_{j+1}^-) &= \left(-\frac{\pi}{2}\right)^4[8(2 + s(\xi))a_j]. \\ F^v_j(n_{j+1}^-) &= \left(\frac{\pi}{2}\right)^5[(2s(\xi) - 59)a_j]. \end{aligned}$$

The above derivatives are at the same knot n_j^+ . It is clearly evaluated that all other derivative vanishes at this knot except the fourth derivative.

$$F^{iv}_j(n_j^+) = \left(\frac{\pi}{2}\right)^4[(6 + 6s(\xi))a_j]. \tag{A3}$$

In the knot interval $n \in [n_{j+1}, n_{j+2})$, the derivatives are taken at knot n_{j+1}^+ as:

$$\begin{aligned}
 F_j(n_{j+1}^+) &= s(\xi)(c_{j+1,0} + c_{j+1,2}) + 4(s(\xi) + 1)c_{j+1,1}. \\
 F_j'(n_{j+1}^+) &= \left(\frac{\pi}{2}\right)(1 + 2s(\xi))(c_{j+1,2} - c_{j+1,0}). \\
 F_j''(n_{j+1}^+) &= \left(\frac{\pi}{2}\right)^2(2(2 + s(\xi)))(c_{j+1,0} - 2c_{j+1,1} + c_{j+1,2}). \\
 F_j'''(n_{j+1}^+) &= \left(\frac{\pi}{2}\right)^3(2s(\xi) - 5)(c_{j+1,0} - c_{j+1,2}). \\
 F_j^{iv}(n_{j+1}^+) &= \left(-\frac{\pi}{2}\right)^4[8(2 + s(\xi))(c_{j+1,0} - c_{j+1,1} + c_{j+1,2} - c_{j+1,3}) - 2(s(\xi) + 11)(c_{j+1,1} - c_{j+1,3})]. \\
 F_j^v(n_{j+1}^+) &= \left(-\frac{\pi}{2}\right)^5[(2s(\xi) - 59)(c_{j+1,0} - c_{j+1,2})].
 \end{aligned}$$

Derivatives at knot n_{j+2}^- are:

$$\begin{aligned}
 F_j(n_{j+2}^-) &= s(\xi)(c_{j+1,1} + c_{j+1,3}) + 4(s(\xi) + 1)c_{j+1,2}. \\
 F_j'(n_{j+2}^-) &= \left(\frac{\pi}{2}\right)(1 + 2s(\xi))(c_{j+1,3} - c_{j+1,1}). \\
 F_j''(n_{j+2}^-) &= \left(\frac{\pi}{2}\right)^2(2(2 + s(\xi)))(c_{j+1,1} - 2c_{j+1,2} + c_{j+1,3}). \\
 F_j'''(n_{j+2}^-) &= \left(\frac{\pi}{2}\right)^3(2s(\xi) - 5)(c_{j+1,1} - c_{j+1,3}). \\
 F_j^{iv}(n_{j+2}^-) &= \left(-\frac{\pi}{2}\right)^4[8(2 + s(\xi))(c_{j+1,3} - c_{j+1,2} - c_{j+1,0}) - 2(s(\xi) + 11)(c_{j+1,2} - c_{j+1,0})]. \\
 F_j^v(n_{j+2}^-) &= \left(-\frac{\pi}{2}\right)^5[(2s(\xi) - 59)(c_{j+1,1} - c_{j+1,3})].
 \end{aligned}$$

In the knot interval $n \in [n_{j+2}, n_{j+3})$, the derivatives are taken at knot n_{j+2}^+ as:

$$\begin{aligned}
 F_j(n_{j+2}^+) &= s(\xi)(b_{j+2,0} + b_{j+2,2}) + 4(s(\xi) + 1)b_{j+2,1}. \\
 F_j'(n_{j+2}^+) &= \left(\frac{\pi}{2}\right)(1 + 2s(\xi))(b_{j+2,2} - b_{j+2,0}). \\
 F_j''(n_{j+2}^+) &= \left(\frac{\pi}{2}\right)^2(2(2 + s(\xi)))(b_{j+2,0} - 2b_{j+2,1} + b_{j+2,2}). \\
 F_j'''(n_{j+2}^+) &= \left(\frac{\pi}{2}\right)^3(2s(\xi) - 5)(b_{j+2,0} - b_{j+2,2}). \\
 F_j^{iv}(n_{j+2}^+) &= \left(\frac{\pi}{2}\right)^4[8(2 + s(\xi))(b_{j+2,1} - b_{j+2,0} - b_{j+2,2} + b_{j+2,3}) + 2(s(\xi) + 11)(b_{j+2,1} - b_{j+2,3})]. \\
 F_j^v(n_{j+2}^+) &= \left(\frac{\pi}{2}\right)^5[(2s(\xi) - 59)(b_{j+2,2} - b_{j+2,0})].
 \end{aligned}$$

Derivatives at knot n_{j+3}^- are:

$$\begin{aligned}
 F_j(n_{j+3}^-) &= s(\xi)(b_{j+2,1} + b_{j+2,3}) + 4(s(\xi) + 1)b_{j+2,2}. \\
 F_j'(n_{j+3}^-) &= \left(\frac{\pi}{2}\right)(1 + 2s(\xi))(b_{j+2,3} - b_{j+2,1}). \\
 F_j''(n_{j+3}^-) &= \left(\frac{\pi}{2}\right)^2(2(2 + s(\xi)))(b_{j+2,1} - 2b_{j+2,2} + b_{j+2,3}). \\
 F_j'''(n_{j+3}^-) &= \left(\frac{\pi}{2}\right)^3(2s(\xi) - 5)(b_{j+2,1} - b_{j+2,3}). \\
 F_j^{iv}(n_{j+3}^-) &= \left(\frac{\pi}{2}\right)^4[8(2 + s(\xi))(b_{j+2,0} - b_{j+2,1} + b_{j+2,2} - b_{j+2,3}) + 2(s(\xi) + 11)(b_{j+2,2} - b_{j+2,0})]. \\
 F_j^v(n_{j+3}^-) &= \left(\frac{\pi}{2}\right)^5[(2s(\xi) - 59)(b_{j+2,3} - b_{j+2,1})].
 \end{aligned}$$

In the knot interval $n \in [n_{j+3}, n_{j+4})$, the derivatives are taken at knot n_{j+3}^+ as:

$$\begin{aligned}
 F_j(n_{j+3}^+) &= s(\xi)d_{j+3}. \\
 F_j'(n_{j+3}^+) &= \left(-\frac{\pi}{2}\right)(1 + 2s(\xi))d_{j+3}. \\
 F_j''(n_{j+3}^+) &= \left(\frac{\pi}{2}\right)^2(2(2 + s(\xi)))d_{j+3}. \\
 F_j'''(n_{j+3}^+) &= \left(\frac{\pi}{2}\right)^3(2s(\xi) - 5)d_{j+3}. \\
 F_j^{iv}(n_{j+3}^+) &= \left(-\frac{\pi}{2}\right)^4[8(2 + s(\xi))d_{j+3}]. \\
 F_j^v(n_{j+3}^+) &= \left(\frac{\pi}{2}\right)^5[(59 - 2s(\xi))d_{j+3}].
 \end{aligned}$$

□

Appendix D

Proof. The derivatives at knot n_j^+ are evaluated as:

$$\begin{aligned} T(n_j^+) &= s(\xi)d_jS_0 + [s(\xi)b_{j,0} + 4(s(\xi) + 1)b_{j,1} + s(\xi)b_{j,2}]S_1, \\ &+ [s(\xi)c_{j,0} + 4(s(\xi) + 1)c_{j,1} + s(\xi)c_{j,2}]S_2, \\ T_j'(n_j^+) &= \left(\frac{\pi}{2}\right)\{(1 + 2s(\xi))[-d_jS_0 + (b_{j,2} - b_{j,0})S_1 + (c_{j,2} - c_{j,0})S_2]\}, \end{aligned}$$

$$T_j''(n_j^+) = \left(\frac{\pi}{2}\right)^2\{2((2 + s(\xi)))[d_jS_0 + (b_{j,0} - 2b_{j,1} + b_{j,2})S_1 + (c_{j,0} - 2c_{j,1} + c_{j,2})S_2]\},$$

$$T_j'''(n_j^+) = \left(\frac{\pi}{2}\right)^3\{(5 + 2s(\xi))[d_jS_0 + (b_{j,0} - b_{j,2})S_1 + (c_{j,0} - c_{j,2})S_2]\},$$

$$\begin{aligned} T_j^{iv}(n_j^+) &= -\left(\frac{\pi}{2}\right)^4\{[8(2 + s(\xi))(d_jS_0 + (b_{j,0} - b_{j,1} + b_{j,2} - b_{j,3})S_1 + (c_{j,0} - c_{j,1} + c_{j,2} - c_{j,3})S_2 + a_jS_3) \\ &+ 2(s(\xi) + 11)[(b_{j,1} - b_{j,3})S_1 + (c_{j,1} - c_{j,3})S_2 - a_jS_3]\}, \end{aligned}$$

$$T_j^v(n_j^+) = -\left(\frac{\pi}{2}\right)^5\{[(59 - 2s(\xi))(d_jS_0 + (b_{j,0} - b_{j,2})S_1 + (c_{j,0} - c_{j,2} + c_{j,2})S_2)]\},$$

where $s(\xi) = \xi^2 - \xi + 1$.

The derivatives at knot n_{j+1}^- are evaluated as:

$$\begin{aligned} T(n_{j+1}^-) &= [s(\xi)b_{j,1} + 4(s(\xi) + 1)b_{j,2} + s(\xi)b_{j,3}]S_1 + [s(\xi)c_{j,1} + 4(s(\xi) + 1)c_{j,2} + s(\xi)c_{j,3}]S_2 \\ &+ s(\xi)a_jS_3, \end{aligned}$$

$$T_j'(n_{j+1}^-) = \left(\frac{\pi}{2}\right)\{(1 + 2s(\xi))[(b_{j,3} - b_{j,1})S_1 + (c_{j,3} - c_{j,1})S_2 + a_jS_3]\},$$

$$T_{j+1}''(n_j^-) = \left(\frac{\pi}{2}\right)^2\{2((2 + s(\xi)))[(b_{j,1} - 2b_{j,2} + b_{j,3})S_1 + (c_{j,1} - 2c_{j,2} + c_{j,3})S_2 + a_jS_3]\},$$

$$T_j'''(n_{j+1}^-) = \left(\frac{\pi}{2}\right)^3\{(1 + 2s(\xi))[(b_{j,1} - b_{j,3})S_1 + (c_{j,1} - c_{j,3})S_2 + a_jS_3]\},$$

$$\begin{aligned} T_j^{iv}(n_{j+1}^-) &= \left(\frac{\pi}{2}\right)^4\{[8(2 + s(\xi))(d_jS_0 + (b_{j,0} - b_{j,1} + b_{j,2} - b_{j,3})S_1 + (c_{j,0} - c_{j,1} + c_{j,2} - c_{j,3})S_2 - a_jS_3) \\ &+ 2(s(\xi) + 11)[d_jS_0 + (b_{j,2} - b_{j,0})S_1 + (c_{j,2} - c_{j,0})S_2]\}, \end{aligned}$$

$$T_j^v(n_{j+1}^-) = \left(\frac{\pi}{2}\right)^5\{[(2s(\xi) - 59)((b_{j,3} - b_{j,1})S_1 + (c_{j,3} - c_{j,1})S_2) + a_jS_3]\}.$$

□

Appendix E

Proof. The continuity for knot interval $n \in [n_j, n_{j+1})$ is derived as:

1. Continuity of NURBS curve

At knot n_j^+

$$Q_0(n_j^+) = \frac{s(\xi)d_jw_0H_0}{s(\xi)d_jw_0 + [s(\xi)(b_{j,0} + b_{j,2}) + 4(s(\xi) + 1)b_{j,1}]w_1 + [s(\xi)(c_{j,0} + c_{j,2}) + 4(s(\xi) + 1)c_{j,1}]w_2}. \tag{A4}$$

$$Q_1(n_j^+) = \frac{s(\xi)(b_{j0} + b_{j2}) + 4(s(\xi) + 1)b_{j1}w_1H_1}{s(\xi)d_jw_0 + [s(\xi)(b_{j0} + b_{j2}) + 4(s(\xi) + 1)b_{j1}]w_1 + [s(\xi)(c_{j0} + c_{j2}) + 4(s(\xi) + 1)c_{j1}]w_2}. \tag{A5}$$

$$Q_2(n_j^+) = \frac{s(\xi)(c_{j0} + c_{j2}) + 4(s(\xi) + 1)c_{j1}w_2H_2}{s(\xi)d_jw_0 + [s(\xi)(b_{j0} + b_{j2}) + 4(s(\xi) + 1)b_{j1}]w_1 + [s(\xi)(c_{j0} + c_{j2}) + 4(s(\xi) + 1)c_{j1}]w_2}. \tag{A6}$$

$$Q_3(n_j^+) = 0. \tag{A7}$$

At knot n_{j+1}^-

$$Q_0(n_{j+1}^-) = 0. \tag{A8}$$

$$Q_1(n_{j+1}^-) = \frac{[s(\xi)(b_{j1} + b_{j3}) + 4(s(\xi) + 1)b_{j2}]w_1H_1}{[s(\xi)(b_{j1} + b_{j3}) + 4(s(\xi) + 1)b_{j2}]w_1 + [s(\xi)(c_{j1} + c_{j3}) + 4(s(\xi) + 1)c_{j2}]w_2 + s(\xi)a_jw_3}. \tag{A9}$$

$$Q_2(n_{j+1}^-) = \frac{[s(\xi)(c_{j1} + c_{j3}) + 4(s(\xi) + 1)c_{j2}]w_2H_2}{[s(\xi)(b_{j1} + b_{j3}) + 4(s(\xi) + 1)b_{j2}]w_1 + [s(\xi)(c_{j1} + c_{j3}) + 4(s(\xi) + 1)c_{j2}]w_2 + s(\xi)a_jw_3}. \tag{A10}$$

$$Q_3(n_{j+1}^-) = \frac{s(\xi)a_jw_3H_3}{[s(\xi)(b_{j1} + b_{j3}) + 4(s(\xi) + 1)b_{j2}]w_1 + [s(\xi)(c_{j1} + c_{j3}) + 4(s(\xi) + 1)c_{j2}]w_2 + s(\xi)a_jw_3}. \tag{A11}$$

First derivative at knot n_j^+

Let $A = s(\xi)d_jw_0 + [s(\xi)(b_{j0} + b_{j2}) + 4(s(\xi) + 1)b_{j1}]w_1 + [s(\xi)(c_{j0} + c_{j2}) + 4(s(\xi) + 1)c_{j1}]w_2$.

$$Q'_0(n_j^+) = \frac{[-\frac{\pi}{2q_j}](1 + 2s(\xi))[A + s(\xi)(-d_jw_0 + (b_{j2} - b_{j0})w_1 + (c_{j2} - c_{j0})w_2)]d_jw_0H_0}{A^2}. \tag{A12}$$

$$Q'_1(n_j^+) = \left(\frac{\pi}{2q_j}\right)(1 + 2s(\xi)) \left[\frac{(b_{j2} - b_{j0})A - [s(\xi)(b_{j0} + b_{j2}) + 4(s(\xi) + 1)b_{j1}]}{[-d_jw_0 + (b_{j2} - b_{j0})w_1 + (c_{j2} - c_{j0})w_2]} \right] w_1H_1. \tag{A13}$$

$$Q'_2(n_j^+) = \left(\frac{\pi}{2q_j}\right)(1 + 2s(\xi)) \left[\frac{(c_{j2} - c_{j0})A - [s(\xi)(c_{j0} + c_{j2}) + 4(s(\xi) + 1)c_{j1}]}{[-d_jw_0 + (b_{j2} - b_{j0})w_1 + (c_{j2} - c_{j0})w_2]} \right] w_2H_2. \tag{A14}$$

$$Q'_3(n_j^+) = 0. \tag{A15}$$

First derivative at knot n_{j+1}^-

$B = [s(\xi)(b_{j1} + b_{j3}) + 4(s(\xi) + 1)b_{j2}]w_1 + [s(\xi)(c_{j1} + c_{j3}) + 4(s(\xi) + 1)c_{j2}]w_2 + s(\xi)a_jw_3$.

$$Q'_0(n_{j+1}^-) = 0. \tag{A16}$$

$$Q'_1(n_{j+1}^-) = \left(\frac{\pi}{2q_j}\right)(1 + 2s(\xi)) \left[\frac{(b_{j3} - b_{j1})B - [s(\xi)(b_{j1} + b_{j3}) + 4(s(\xi) + 1)b_{j2}]}{[(b_{j3} - b_{j1})w_1 + (c_{j3} - c_{j1})w_2 + a_jw_3]} \right] w_1H_1. \tag{A17}$$

$$Q'_2(n_{j+1}^-) = \left(\frac{\pi}{2q_j}\right)(1 + 2s(\xi)) \left[\frac{(c_{j3} - c_{j1})B - [s(\xi)(c_{j1} + c_{j3}) + 4(s(\xi) + 1)c_{j2}]}{[(b_{j3} - b_{j1})w_1 + (c_{j3} - c_{j1})w_2 + a_jw_3]} \right] w_2H_2. \tag{A18}$$

$$Q'_3(n_{j+1}^-) = \frac{[\frac{\pi}{2q_j}](1 + 2s(\xi))[B - s(\xi)((b_{j3} - b_{j1})w_1 + (c_{j3} - c_{j1})w_2 + a_jw_3)]a_jw_3H_3}{B^2}. \tag{A19}$$

Second derivative at knot n_j^+

$$Q_0''(n_j^+) = \left(\frac{\pi}{2q_j}\right)^2(2s(\xi) + 2) \left[\frac{A^- [s(\xi)(2s(\xi) - 5)(d_j w_0 + (b_{j0} - b_{j2})w_1 + (c_{j0} - c_{j2})w_2)]}{A^2} \right] d_j w_0 H_0$$

$$+ 2\left(\frac{\pi}{2q_j}\right)^2(1 + 2s(\xi)) \left[\frac{[-d_j w_0 + (b_{j2} - b_{j0})w_1 + (c_{j2} - c_{j0})w_2]}{[A + [s(\xi)(-d_j w_0 + (b_{j2} - b_{j0})w_1 + (c_{j2} - c_{j0})w_2)]]} \right] d_j w_0 H_0. \tag{A20}$$

$$Q_1''(n_j^+) = \left(\frac{\pi}{2q_j}\right)^2(2s(\xi) + 2) \left[\frac{A[b_{j0} - 2b_{j1} + b_{j2}] - J[s(\xi)(b_{j0} + b_{j2}) + 4(s(\xi) + 1)b_{j1}]}{A^2} \right] w_1 H_1$$

$$- 2\left(\frac{\pi}{2q_j}\right)^2(1 + 2s(\xi)) M \left[\frac{A[(1 + 2s(\xi))(b_{j2} - b_{j0})]}{[M[s(\xi)(b_{j0} + b_{j2}) + 4(s(\xi) + 1)b_{j1}]]} \right] w_1 H_1. \tag{A21}$$

$$Q_2''(n_j^+) = \left(\frac{\pi}{2q_j}\right)^2(2s(\xi) + 2) \left[\frac{A[c_{j0} - 2c_{j1} + c_{j2}] - [s(\xi)(c_{j0} + c_{j2}) + 4(s(\xi) + 1)c_{j1}]J}{A^2} \right] w_2 H_2$$

$$- 2\left(\frac{\pi}{2q_j}\right)^2(1 + 2s(\xi)) M \left[\frac{A[(1 + 2s(\xi))(c_{j2} - c_{j0})]}{[M[s(\xi)(c_{j0} + c_{j2}) + 4(s(\xi) + 1)c_{j1}]]} \right] w_2 H_2. \tag{A22}$$

$$Q_3''(n_j^+) = 0. \tag{A23}$$

where $J = d_j w_0 + (b_{j0} - 2b_{j1} + b_{j2})w_1 + (c_{j0} - 2c_{j1} + c_{j2})w_2$ and $M = -d_j w_0 + (b_{j2} - b_{j0})w_1 + (c_{j2} - c_{j0})w_2$.

Second derivative at knot n_{j+1}^-

Let $K = (b_{j1} - 2(b_{j2}) + b_{j3})w_1 + (c_{j1} - 2(c_{j2}) + c_{j3})w_2 + a_j w_3$ and $L = (b_{j3} - b_{j1})w_1 + (c_{j3} - c_{j1})w_2 + a_j w_3$.

$$Q_0''(n_{j+1}^-) = 0. \tag{A24}$$

$$Q_1''(n_{j+1}^-) = \left(\frac{\pi}{2q_j}\right)^2(2s(\xi) + 2) \left[\frac{B[b_{j1} - 2b_{j2} + b_{j3}] - K[s(\xi)(b_{j1} + b_{j3}) + 4(s(\xi) + 1)b_{j2}]}{B^2} \right] w_1 H_1$$

$$- 2\left(\frac{\pi}{2q_j}\right)^2(1 + 2s(\xi)) L \left[\frac{B[(1 + 2s(\xi))(b_{j3} - b_{j1})]}{[L[s(\xi)(b_{j1} + b_{j3}) + 4(s(\xi) + 1)b_{j2}]]} \right] w_1 H_1. \tag{A25}$$

$$Q_2''(n_{j+1}^-) = \left(\frac{\pi}{2q_j}\right)^2(2s(\xi) + 2) \left[\frac{B[c_{j1} - 2c_{j2} + c_{j3}] - K[s(\xi)(c_{j1} + c_{j3}) + 4(s(\xi) + 1)c_{j2}]}{B^2} \right] w_2 H_2$$

$$- 2\left(\frac{\pi}{2q_j}\right)^2(1 + 2s(\xi)) L \left[\frac{B[(1 + 2s(\xi))(c_{j3} - c_{j1})]}{[L[s(\xi)(c_{j1} + c_{j3}) + 4(s(\xi) + 1)c_{j2}]]} \right] w_2 H_2. \tag{A26}$$

$$Q_3''(n_{j+1}^-) = \left(\frac{\pi}{2q_j}\right)^2(2s(\xi) + 2) \left[\frac{B^- [s(\xi)(2s(\xi) - 5)][(b_{j1} - b_{j3})w_1 + (c_{j1} - c_{j3})w_2 + a_j w_3]}{B^2} \right] a_j w_3 H_3$$

$$- 2\left(\frac{\pi}{2q_j}\right)^2(1 + 2s(\xi)) L \left[\frac{B - [s(\xi)L]}{B^3} \right] a_j w_3 H_3. \tag{A27}$$

Third derivative at knot n_j^+

Let $m(\xi)^2 = (1 + 2s(\xi))2(2 + s(\xi))$, $g(\xi) = 2(2s(\xi) - 5)$ and $e(\xi) = (1 + 2s(\xi))^3$.

$$\begin{aligned}
 Q_0'''(n_j^+) &= \left(\frac{\pi}{2q_j}\right)^3 g(\xi) d_j w_0 H_0 \left[\frac{[(s(\xi)b_{j2} + 2(s(\xi) + 1)b_{j1})w_1 + (s(\xi)c_{j2} + 2(s(\xi) + 1)c_{j1})w_2] + [4(2s(\xi) + 1)(s(\xi) + 2)[(b_{j2} - b_{j1})w_1 + (c_{j2} - c_{j1})w_2]]}{A^2} \right. \\
 &\quad \left. - 8\left(\frac{\pi}{2q_j}\right)^3 (s(\xi))^2 d_j w_0 H_0 \left[\frac{(2 + 3s(\xi))M(b_{j1}w_1 + c_{j1}w_2) - 2J[(s(\xi)b_{j2} + 2(s(\xi) + 1)b_{j1})w_1 + (s(\xi)c_{j2} + 2(s(\xi) + 1)c_{j1})w_2]}{A^3} \right] \right. \\
 &\quad \left. - 12\left(\frac{\pi}{2q_j}\right)^3 e(\xi) d_j w_0 H_0 \left[\frac{M[(s(\xi)b_{j2} + 2(s(\xi) + 1)b_{j1})w_1 + (s(\xi)c_{j2} + 2(s(\xi) + 1)c_{j1})w_2]}{A^4} \right] \right]. \tag{A28}
 \end{aligned}$$

$$\begin{aligned}
 Q_1'''(n_j^+) &= \left(\frac{\pi}{2q_j}\right)^3 d_j w_0 w_1 H_1 \left[\frac{[(-2s(\xi)b_{j2} - 4(s(\xi) + 1)b_{j1})(2s(\xi) - 5) - 4(2s(\xi) + 1)(s(\xi) + 2)((b_{j2} - b_{j1}))]}{A^2} \right] \\
 &\quad - 2\left(\frac{\pi}{2q_j}\right)^3 \left[\frac{2M[A(b_{j0} - 2b_{j1} + b_{j2}) - (s(\xi)(b_{j0} + b_{j2}) + 4(s(\xi) + 1)b_{j1})J] - 2J[A(b_{j2} - b_{j0}) - (s(\xi)(b_{j0} + b_{j2}) + 4(s(\xi) + 1)b_{j1})M]}{A^3} \right] w_1 H_1 \tag{A29}
 \end{aligned}$$

$$+ 6\left(\frac{\pi}{2q_j}\right)^3 (1 + 2s(\xi))^3 M^2 \left[\frac{[A(b_{j2} - b_{j0}) - (s(\xi)(b_{j0} + b_{j2}) + 4(s(\xi) + 1)b_{j1})M]}{A^3} \right] w_1 H_1.$$

$$\begin{aligned}
 Q_2'''(n_j^+) &= \left(\frac{\pi}{2q_j}\right)^3 d_j w_0 w_2 H_2 \left[\frac{[(-2s(\xi)c_{j2} - 4(s(\xi) + 1)c_{j1})(2s(\xi) - 5) - 4(2s(\xi) + 1)(s(\xi) + 2)((c_{j2} - c_{j1}))]}{A^2} \right] \\
 &\quad - 2\left(\frac{\pi}{2q_j}\right)^3 \left[\frac{2M[A(c_{j0} - 2c_{j1} + c_{j2}) - (s(\xi)(c_{j0} + c_{j2}) + 4(s(\xi) + 1)c_{j1})J] - 2J[A(c_{j2} - c_{j0}) - (s(\xi)(c_{j0} + c_{j2}) + 4(s(\xi) + 1)c_{j1})M]}{A^3} \right] w_2 H_2 \tag{A30}
 \end{aligned}$$

$$+ 6\left(\frac{\pi}{2q_j}\right)^3 (1 + 2s(\xi))^3 M^2 \left[\frac{[A(c_{j2} - c_{j0}) - (s(\xi)(c_{j0} + c_{j2}) + 4(s(\xi) + 1)c_{j1})M]}{A^4} \right] w_2 H_2.$$

$$Q_3'''(n_j^+) = 0. \tag{A31}$$

Third derivative at knot n_{j+1}^-

$$Q_0'''(n_{j+1}^-) = 0. \tag{A32}$$

$$\begin{aligned}
 Q_1'''(n_{j+1}^-) &= \left(\frac{\pi}{2q_j}\right)^3 a_j w_3 w_1 H_1 \left[\frac{[(-2s(\xi)b_{j3} - 4(s(\xi) + 1)b_{j2})(2s(\xi) - 5) + 4(2s(\xi) + 1)(s(\xi) + 2)((b_{j1} - b_{j2}))]}{B^2} \right] \\
 &\quad - 2\left(\frac{\pi}{2q_j}\right)^3 \left[\frac{2L[B(b_{j1} - 2b_{j2} + b_{j3}) - (s(\xi)(b_{j1} + b_{j3}) + 4(s(\xi) + 1)b_{j2})K] - 2K[B(b_{j3} - b_{j1}) - (s(\xi)(b_{j1} + b_{j3}) + 4(s(\xi) + 1)b_{j2})L]}{B^3} \right] w_1 H_1 \tag{A33}
 \end{aligned}$$

$$+ 6\left(\frac{\pi}{2q_j}\right)^3 (1 + 2s(\xi))^3 L^2 \left[\frac{[B(b_{j3} - b_{j1}) - (s(\xi)(b_{j1} + b_{j3}) + 4(s(\xi) + 1)b_{j2})L]}{B^4} \right] w_1 H_1.$$

$$\begin{aligned}
 Q_2'''(n_{j+1}^-) &= \left(\frac{\pi}{2q_j}\right)^3 a_j w_3 w_2 H_2 \left[\frac{[(-2s(\xi)c_{j3} - 4(s(\xi) + 1)c_{j2})(2s(\xi) - 5) + 4(2s(\xi) + 1)(s(\xi) + 2)((c_{j1} - c_{j2}))]}{B^2} \right] \\
 &\quad - 2\left(\frac{\pi}{2q_j}\right)^3 \left[\frac{2L[B(c_{j1} - 2c_{j2} + c_{j3}) - [(s(\xi)(c_{j1} + c_{j3}) + 4(s(\xi) + 1)c_{j2})K]] - 2K[B(c_{j3} - c_{j1}) - (s(\xi)(c_{j1} + c_{j3}) + 4(s(\xi) + 1)c_{j2})L]}{B^3} \right] w_2 H_2 \quad (A34) \\
 &\quad + 6\left(\frac{\pi}{2q_j}\right)^3 (1 + 2s(\xi))^3 L^2 \left[\frac{[B(c_{j3} - c_{j1}) - (s(\xi)(c_{j1} + c_{j3}) + 4(s(\xi) + 1)c_{j2})L]}{B^4} \right] w_2 H_2.
 \end{aligned}$$

$$\begin{aligned}
 Q_3'''(n_{j+1}^-) &= \left(\frac{\pi}{2q_j}\right)^3 g(\xi) a_j w_3 H_3 \left[\frac{[(s(\xi)b_{j3} + 2(s(\xi) + 1)b_{j2})w_1 + (s(\xi)c_{j3} + 2(s(\xi) + 1)c_{j2})w_2] + [4(2s(\xi) + 1)(s(\xi) + 2)[(b_{j3} - b_{j2})w_1 + (c_{j3} - c_{j2})w_2]}{B^2} \right] \\
 &\quad - 8\left(\frac{\pi}{2q_j}\right)^3 (s(\xi))^2 a_j w_3 H_3 \left[\frac{(2 + 3s(\xi))L(b_{j2}w_1 + c_{j2}w_2) - 2K[(s(\xi)b_{j3} + 2(s(\xi) + 1)b_{j2})w_1 + (s(\xi)c_{j3} + 2(s(\xi) + 1)c_{j2})w_2]}{B^3} \right] \quad (A35) \\
 &\quad - 12\left(\frac{\pi}{2q_j}\right)^3 e(\xi) a_j w_3 H_3 \left[\frac{L[(s(\xi)b_{j3} + 2(s(\xi) + 1)b_{j2})w_1 + (s(\xi)c_{j3} + 2(s(\xi) + 1)c_{j2})w_2]}{B^4} \right].
 \end{aligned}$$

2. Continuity of Rational trigonometric B-spline curve

At knot n_j^+ .

$$Q_0(n_j^+) = \frac{s(\xi)w_0H_0}{[s(\xi)(w_0 + w_2) + 4(s(\xi) + 1)w_1]}. \quad (A36)$$

$$Q_1(n_j^+) = \frac{4(s(\xi) + 1)w_1H_1}{[s(\xi)(w_0 + w_2) + 4(s(\xi) + 1)w_1]}. \quad (A37)$$

$$Q_2(n_j^+) = \frac{4(s(\xi) + 1)w_2H_2}{[s(\xi)(w_0 + w_2) + 4(s(\xi) + 1)w_1]}. \quad (A38)$$

$$Q_3(n_j^+) = 0. \quad (A39)$$

At knot n_{j+1}^-

$$Q_0(n_{j+1}^-) = 0. \quad (A40)$$

$$Q_1(n_{j+1}^-) = \frac{4(s(\xi) + 1)w_1H_1}{[s(\xi)(w_1 + w_3) + 4(s(\xi) + 1)w_2]}. \quad (A41)$$

$$Q_2(n_{j+1}^-) = \frac{4(s(\xi) + 1)w_2H_2}{[s(\xi)(w_1 + w_3) + 4(s(\xi) + 1)w_2]}. \quad (A42)$$

$$Q_3(n_{j+1}^-) = \frac{(s(\xi))w_3H_3}{[s(\xi)(w_1 + w_3) + 4(s(\xi) + 1)w_2]}. \quad (A43)$$

First derivative at knot n_j^+

$$Q_0'(n_j^+) = \left(-\frac{\pi}{2q_j}\right)(1 + 2s(\xi)) \left[\frac{s(\xi)(w_0 + w_2) + 4(s(\xi) + 1)w_1 + s(\xi)(-w_0 + w_2)}{[s(\xi)(w_0 + w_2) + 4(s(\xi) + 1)w_1]^2} \right] w_0 H_0. \quad (A44)$$

$$Q_1'(n_j^+) = \left(\frac{\pi}{2}\right) \left[\frac{(1 + 2s(\xi))[-4(s(\xi) + 1)(-w_0 + w_2)]w_1 H_1}{[s(\xi)(w_0 + w_2) + 4(s(\xi) + 1)w_1]^2} \right]. \quad (A45)$$

$$Q'_2(n_j^+) = \left(\frac{\pi}{2q_j}\right)(1 + 2s(\xi)) \left[\frac{s(\xi)(w_0 + w_2) + 4(s(\xi) + 1)w_1 - s(\xi)(-w_0 + w_2)}{[s(\xi)(w_0 + w_2) + 4(s(\xi) + 1)w_1]^2} \right] w_2 H_2. \tag{A46}$$

$$Q_3(n_j^+) = 0 \tag{A47}$$

First derivative at knot n_{j+1}^-

$$Q_0(n_{j+1}^-) = 0 \tag{A48}$$

$$Q'_1(n_{j+1}^-) = \left(\frac{\pi}{2q_j}\right)(1 + 2s(\xi)) \left[\frac{s(\xi)(w_1 + w_3) + 4(s(\xi) + 1)w_2 - s(\xi)(-w_1 + w_3)}{[s(\xi)(w_1 + w_3) + 4(s(\xi) + 1)w_2]^2} \right] w_1 H_1. \tag{A49}$$

$$Q'_2(n_{j+1}^-) = \left(\frac{\pi}{2}\right) \left[\frac{(1 + 2s(\xi))[-4(s(\xi) + 1)(-w_1 + w_3)]w_2 H_2}{[s(\xi)(w_1 + w_3) + 4(s(\xi) + 1)w_2]^2} \right]. \tag{A50}$$

$$Q'_3(n_{j+1}^-) = \left(\frac{\pi}{2q_j}\right)(1 + 2s(\xi)) \left[\frac{s(\xi)(w_1 + w_3) + 4(s(\xi) + 1)w_2 - s(\xi)(-w_1 + w_3)}{[s(\xi)(w_1 + w_3) + 4(s(\xi) + 1)w_2]^2} \right] w_3 H_3. \tag{A51}$$

Second derivative at knot n_j^+

$$Q''_0(n_j^+) = \left(\frac{\pi}{2q_j}\right)^2 (2(s(\xi) + 2)) \left[\frac{s(\xi)(w_0 + w_2) + 4(s(\xi) + 1)w_1 - s(\xi)[(2s(\xi) - 5)(w_0 - w_2)]}{[s(\xi)(w_0 + w_2) + 4(s(\xi) + 1)w_1]^2} \right] w_0 H_0 \tag{A52}$$

$$+ 2\left(\frac{\pi}{2q_j}\right)^2 (1 + 2s(\xi))(-w_0 + w_2) \left[\frac{s(\xi)(w_0 + w_2) + 4(s(\xi) + 1)w_1 - s(\xi)(-w_0 + w_2)}{[s(\xi)(w_0 + w_2) + 4(s(\xi) + 1)w_1]^3} \right] w_0 H_0.$$

$$Q''_1(n_j^+) = \left(\frac{\pi}{2q_j}\right)^2 (2(s(\xi) + 2)) \left[\frac{-2[s(\xi)(w_0 + w_2) + 4(s(\xi) + 1)w_1] - 4(s(\xi) + 1)[(w_0 - 2w_1 + w_2)]}{[s(\xi)(w_0 + w_2) + 4(s(\xi) + 1)w_1]^2} \right] w_1 H_1 \tag{A53}$$

$$- 2\left(\frac{\pi}{2q_j}\right)^2 (1 + 2s(\xi))(-w_0 + w_2) \left[\frac{-4(s(\xi) + 1)(-w_0 + w_2)}{[s(\xi)(w_0 + w_2) + 4(s(\xi) + 1)w_1]^3} \right] w_1 H_1.$$

$$Q''_2(n_j^+) = \left(\frac{\pi}{2q_j}\right)^2 (2(s(\xi) + 2)) \left[\frac{[s(\xi)(w_0 + w_2) + 4(s(\xi) + 1)w_1] - s(\xi)[(w_0 - 2w_1 + w_2)]}{[s(\xi)(w_0 + w_2) + 4(s(\xi) + 1)w_1]^2} \right] w_2 H_2 \tag{A54}$$

$$- 2\left(\frac{\pi}{2q_j}\right)^2 (1 + 2s(\xi))(-w_0 + w_2) \left[\frac{[s(\xi)(w_0 + w_2) + 4(s(\xi) + 1)w_1]}{[s(\xi)(w_0 + w_2) + 4(s(\xi) + 1)w_1]^3} \right] w_2 H_2.$$

$$Q''_2(n_j^+) = 0. \tag{A55}$$

Second derivative at knot n_{j+1}^-

$$Q''_0(n_{j+1}^-) = 0. \tag{A56}$$

$$\begin{aligned}
 Q_1''(n_{j+1}^-) &= \left(\frac{\pi}{2q_j}\right)^2(2(s(\xi) + 2)) \left[\frac{[s(\xi)(w_1 + w_3) + 4(s(\xi) + 1)w_2] - 4(s(\xi) + 1)[(w_1 - 2w_2 + w_3)]}{[s(\xi)(w_1 + w_3) + 4(s(\xi) + 1)w_2]^2} \right] w_1 H_1 \\
 &\quad - 2\left(\frac{\pi}{2q_j}\right)^2(1 + 2s(\xi))(-w_1 + w_3) \left[\frac{[s(\xi)(w_1 + w_3) + 4(s(\xi) + 1)w_2] - [(-1 + 2s(\xi)) - (s(\xi)(-w_1 + w_3))]}{[s(\xi)(w_1 + w_3) + 4(s(\xi) + 1)w_2]^3} \right] w_1 H_1.
 \end{aligned}
 \tag{A57}$$

$$\begin{aligned}
 Q_2''(n_{j+1}^-) &= \left(\frac{\pi}{2q_j}\right)^2(2(s(\xi) + 2)) \left[\frac{-2[s(\xi)(w_3 + w_1) + 4(s(\xi) + 1)w_2] - 4(s(\xi) + 1)[(w_1 - 2w_2 + w_3)]}{[s(\xi)(w_1 + w_3) + 4(s(\xi) + 1)w_2]^2} \right] w_2 H_2 \\
 &\quad - 2\left(\frac{\pi}{2q_j}\right)^2(1 + 2s(\xi))(-w_1 + w_3) \left[\frac{[4(s(\xi) + 1)(-w_1 + w_3)]}{[s(\xi)(w_1 + w_3) + 4(s(\xi) + 1)w_2]^3} \right] w_2 H_2.
 \end{aligned}
 \tag{A58}$$

$$\begin{aligned}
 Q_3''(n_{j+1}^-) &= \left(\frac{\pi}{2q_j}\right)^2(2(s(\xi) + 2)) \left[\frac{s(\xi)(w_1 + w_3) + 4(s(\xi) + 1)w_2 - s(\xi)[(2s(\xi) - 5)(w_1 + w_3)]}{[s(\xi)(w_1 + w_3) + 4(s(\xi) + 1)w_2]^2} \right] w_3 H_3 \\
 &\quad + 2\left(\frac{\pi}{2q_j}\right)^2(1 + 2s(\xi))(-w_1 + w_3) \left[\frac{s(\xi)(w_1 + w_3) + 4(s(\xi) + 1)w_2 - s(\xi)(-w_1 + w_3)}{[s(\xi)(w_1 + w_3) + 4(s(\xi) + 1)w_2]^3} \right] w_3 H_3.
 \end{aligned}
 \tag{A59}$$

In similar manner, third derivative for uniform knots is evaluated. \square

References

1. Bashir, U.; Abbas, M.; Awang, M.N.H.; Ali, J.M. A class of quasi-quintic trigonometric Bézier curve with two shape parameters. *Sci. Asia* **2013**, *39S*, 11–15. [\[CrossRef\]](#)
2. Bashir, U.; Abbas, M.; Ali, J.M. The G^2 and C^2 rational quadratic trigonometric Bézier curve with two shape parameters with applications. *J. Appl. Math. Comput.* **2013**, *219*, 10183–10197. [\[CrossRef\]](#)
3. BiBi, S.; Abbas, M.; Misro, M.Y.; Hu, G. A Novel Approach of Hybrid Trigonometric Bézier Curve to the Modeling of Symmetric Revolutionary Curves and Symmetric Rotation Surfaces. *IEEE Access.* **2019**, *7*, 165779–165792. [\[CrossRef\]](#)
4. Maqsood, S.; Abbas, M.; Hu, G.; Ramli, A.L.A.; Miura, K.T. A Novel Generalization of Trigonometric Bézier Curve and Surface with Shape Parameters and Its Applications. *Math. Probl. Eng.* **2020**, *2020*, 4036434. [\[CrossRef\]](#)
5. Usman, M.; Abbas, M.; Miura, K.T. Some engineering applications of new trigonometric cubic Bézier-like curves to free-form complex curve modeling. *J. Adv. Mech. Des. Syst. Manuf.* **2020**, *14*, 19-00420. [\[CrossRef\]](#)
6. Hu, X.; Hu, G.; Abbas, M.; Misro, M.Y. Approximate multi-degree reduction of Q-Bézier curves via generalized Bernstein polynomial functions. *Adv. Differ. Equ.* **2020**, *2020*, 1–16. [\[CrossRef\]](#)
7. Li, F.; Hu, G.; Abbas, M.; Miura, K.T. The Generalized H-Bézier Model: Geometric Continuity Conditions and Applications to Curve and Surface Modeling. *Mathematics* **2020**, *8*, 924. [\[CrossRef\]](#)
8. Majeed, A.; Abbas, M.; Miura, K.T.; Kamran, M.; Nazir, T. Surface Modeling from 2D Contours with an Application to Craniofacial Fracture Construction. *Mathematics* **2020**, *8*, 1246. [\[CrossRef\]](#)
9. Hu, G.; Li, H.; Abbas, M.; Miura, K.T.; Wei, G. Explicit Continuity Conditions for G1 Connection of S- λ Curves and Surfaces. *Mathematics* **2020**, *8*, 1359. [\[CrossRef\]](#)
10. Schoenberg, I.J. On trigonometric spline interpolation. *J. Math. Mech.* **1964**, *13*, 795–825.
11. Schoenberg, I.J. Spline interpolation and best quadrature formulae. *Bull. Am. Math. Soc.* **1964**, *70*, 143–148. [\[CrossRef\]](#)
12. Schoenberg, I.J. Spline interpolation and the higher derivatives. *Proc. Natl. Acad. Sci. USA* **1964**, *51*, 24. [\[CrossRef\]](#)

13. Schoenberg, I.J. Interpolating splines as limits of polynomials. *Linear Algebra Appl.* **1983**, *52*, 617–628. [[CrossRef](#)]
14. Lyche, T.; Winther, R. A stable recurrence relation for trigonometric B-splines. *J. Approx. Theory* **1979**, *25*, 266–279. [[CrossRef](#)]
15. Walz, G. Identities for trigonometric B-splines with an application to curve design. *Bit Numer. Math.* **1997**, *37*, 189–201. [[CrossRef](#)]
16. Piegl, L.; Tiller, W. *The NURBS Book*; Springer Science & Business Media: Berlin/Heidelberg, Germany, 2012.
17. Marsh, D. *Applied Geometry for Computer Graphics and CAD*; Springer: Berlin/Heidelberg, Germany, 2006.
18. Salomon, D. *Curves and Surfaces for Computer Graphics*; Springer Science & Business Media: Berlin/Heidelberg, Germany, 2007.
19. Juhász, I.; Róth, Á. A scheme for interpolation with trigonometric spline curves. *J. Comput. Appl. Math.* **2014**, *263*, 246–261. [[CrossRef](#)]
20. Zhu, Y.P.; Han, X.L. New trigonometric basis possessing exponential shape parameters. *J. Comput. Math.* **2015**, *33*, 642–684.
21. Majeed, A.; Qayyum, F. New rational cubic trigonometric B-spline curves with two shape parameters. *Comput. Appl. Math.* **2020**, *39*, 1–24. [[CrossRef](#)]
22. Han, X. Quadratic trigonometric polynomial curves with a shape parameter. *Comput. Aided Geom. Des.* **2002**, *19*, 503–512. [[CrossRef](#)]
23. Han, X. Cubic trigonometric polynomial curves with a shape parameter. *Comput. Aided Geom. Des.* **2004**, *21*, 535–548. [[CrossRef](#)]
24. Majeed, A.; Yahya, Z.R.; Abdullah, J.Y.; Rafique, M. Construction of occipital bone fracture using B-spline curves. *Comput. Appl. Math.* **2018**, *37*, 2877–2896. [[CrossRef](#)]
25. Choubey, N.; Ojha, A. Trigonometric splines with variable shape parameter. *Rocky Mt. J. Math.* **2008**, *38*, 91–105. [[CrossRef](#)]
26. Pagani, L.; Scott, P.J. Curvature based sampling of curves and surfaces. *Comput. Aided Geom. Des.* **2018**, *59*, 32–48. [[CrossRef](#)]
27. Majeed, A.; Mt Piah, A.R.; Yahya, Z.R. Surface reconstruction from parallel curves with application to parietal bone fracture reconstruction. *PLoS ONE* **2016**, *11*, e0149921. [[CrossRef](#)] [[PubMed](#)]
28. Hu, G.; Qin, X.; Ji, X.; Wei, G.; Zhang, S. The construction of $\lambda\mu$ -B-spline curves and its application to rotational surfaces. *Appl. Math. Comput.* **2015**, *266*, 194–211. [[CrossRef](#)]
29. Majeed, A.; Gobithaasan, R.U.; Yahya, Z.R. Craniofacial reconstruction using rational cubic ball curves. *PLoS ONE* **2015**, *10*, e0122854. [[CrossRef](#)] [[PubMed](#)]
30. Yan, L.; Liang, J. A class of algebraic–trigonometric blended splines. *J. Comput. Appl. Math.* **2011**, *235*, 1713–1729. [[CrossRef](#)]
31. Troll, E. Constrained modification of the cubic trigonometric Bézier curve with two shape parameters. *Ann. Math. Inform.* **2014**, *43*, 145–156.
32. Stanimirović, P.S.; Krtolica, P.V.; Saračević, M.H.; Mašović, S.H. Decomposition of Catalan numbers and convex polygon triangulations. *Int. J. Comput. Math.* **2014**, *91*, 1315–1328. [[CrossRef](#)]
33. Saracevic, M.; SELİMÍ, A. Convex polygon triangulation based on planted trivalent binary tree and ballot problem. *Turk. J. Electr. Eng. Comput. Sci.* **2019**, *27*, 346–361. [[CrossRef](#)]
34. Troll, E.M.; Hoffmann, M. Geometric properties and constrained modification of trigonometric spline curves of Han. *Ann. Math. Inform.* **2010**, *37*, 165–175.
35. Han, X.A.; Ma, Y.; Huang, X. The cubic trigonometric Bézier curve with two shape parameters. *Appl. Math. Lett.* **2009**, *22*, 226–231. [[CrossRef](#)]
36. Xu, G.; Wang, G.Z. Extended cubic uniform B-spline and α -B-spline. *Acta Autom. Sin.* **2008**, *34*, 980–984. [[CrossRef](#)]

Publisher’s Note: MDPI stays neutral with regard to jurisdictional claims in published maps and institutional affiliations.



© 2020 by the authors. Licensee MDPI, Basel, Switzerland. This article is an open access article distributed under the terms and conditions of the Creative Commons Attribution (CC BY) license (<http://creativecommons.org/licenses/by/4.0/>).